

A Heavy Mass Energy Storage System Using an AC-DC Linear Machine with Multiple Rotors and Enhanced Lifting Forces

Daming Zhang

School of Electrical Engineering and Telecommunication

University of New South Wales

Australia, 2052

Email: daming.zhang@unsw.edu.au

Abstract—An AC-DC linear machine is designed to lift heavy mass for converting its potential energy to/from electricity. It has the following features: 1) stator structure is interleaved with alternating magnetic and non-magnetic layers; 2) stator windings are wound spreading from the bottom to top of interleaved stator structure; 3) multiple strands of aluminium conductors in the stator windings are in parallel to reduce ohmic losses, leading to higher efficiency; 4) vertical movement of the rotor minimizes friction losses, thereby improving overall efficiency; 5) by using interleaved stator plates, fringing effect is effectively reduced. Such system is environment-friendly and potentially profitable for commercialization. Nevertheless it has relatively long profit-return years. In this paper, a modified topology uses reluctance force to enhance electromagnetic force. Furthermore multiple rotor topologies could be adopted. By doing so, overall lifting force can be increased and the profit return years are shortened.

Keywords—Energy storage; heavy mass; linear machine; vertical movement

I. INTRODUCTION

Potentially re-vamping existing distribution power systems could be beneficial to end users and environment [1-2]. The following reasons are accelerating such progress: 1) in some countries, the prices of electricity have a significant difference at different hours during a day; 2) grid-scale massive energy storage is becoming more and more feasible; 3) urgency of use-up of fossil fuel; 4) anxiety against potential pollution by nuclear fission waste.

Such re-vamping is a part of progress towards future smart grid. The smart grid ideally is formed by many microgrids/grids, each or some of which has the capability to operate in islanded mode.

To cope with intermittence brought by wind energy, solar energy and tidal wave energy etc, grid-scale massive energy storage is indispensable. Currently there are many existing energy storage systems, such as battery storage, hydro-power storage, fly-wheel storage, super-conducting magnetic energy storage, super-capacitor energy storage and heavy mass

energy storage etc[1-6]. Each of them has its pros and cons.

Battery storage is the most convenient one but its price is still quite high. A battery energy storage with 1kWh capability currently costs around 300USD. For massive energy storage, it may not be suitable due to this high price and also its short life span. Furthermore retrieval of battery takes effort and is costly. Pumped-hydro storage using water reservoir is a feasible one only when there is spacious space and water available[1-3].

Although heavy mass energy storage was proposed in [4-6], each method suffers from poor efficiency. In [7], a linear machine has been proposed to convert potential energy of heavy mass to/from electricity. In order to minimize friction losses, it lifts the heavy mass vertically. Furthermore by using multiple parallel aluminium strands to form stator windings, the copper losses in them are reduced, leading to higher efficiency. Moreover, by using transitional pulse current, uplifting force could be increased.

In some applications, such as wind energy storage, the wind may just last several hours during one day. It is necessary to complete the energy storage within that short time span. To solve this problem, in this paper, a multiple rotor structure is adopted to improve the lifting efficacy and increase the storage capability.

To avoid un-smooth movement of the heavy masses along vertical passage due to changing reluctance force, a three-sided or re-configurable rotor topology is proposed as well. Successful operation of such a system depends on effective commutation using carbon brushes.

The following contents are arranged as follows: In Section II, topology of the AC-DC linear machine is introduced; Section III discusses the re-configurable rotor structure; Section IV presents a design with multiple rotors; Conclusion is drawn in Section V.

II. TOPOLOGY OF THE AC-DC LINEAR MACHINE

As described in [7] and shown in Fig. 1a, interleaved magnetic structure of the stator has been taken, where lumped rotor structure is used. Multiple parallel strands of aluminium conductors for the stator spreading from the bottom to the top of the passage

are arranged to reduce the ohmic losses. One may use the poles spreading from the bottom to the top of the passage to support the stator magnetic layer as shown in Fig. 1b. By doing so, alternating non-magnetic layers of the stator can be left as air.

The top and bottom platforms are flat areas where containers sit.

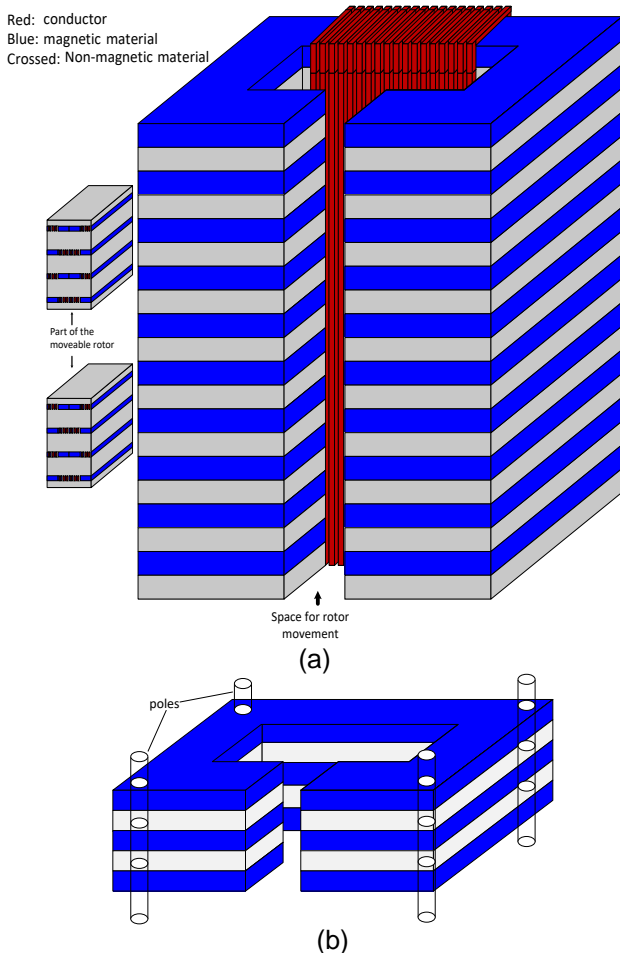


Fig. 1. (a) Stator structure and part of the two sets of lumped rotor structure; (b) Interleaved stator structure with pole supported magnetic layer and non-magnetic air layer

Two possible configurations for rotor conductors are shown in Fig. 2, each one being insulated and embedded or sandwiched in magnetic materials as described in [7]. To reduce the air gap and thereby decrease ampere-turns requirement on the stator winding, flat rotor conductors as shown in Fig. 3b is adopted.

Fig. 3a shows a symmetrical structure in which there are two nearly closed-loop magnetic paths, two identical containers with heavy mass placed symmetrically at two terminals of the container carrier. The two nearly closed-loop magnetic paths are mirror arrangements of the structure as shown in Fig. 1a. There are also reinforcing mechanic parts on the rotors. Fig. 3b shows the magnified basic rotor forming unit composed of rotor conductors embedded or sandwiched in magnetic materials through insulators and mechanic support. To reduce the total

air-gap seen by the stator winding, flat instead of rectangular rotor conductors need be adopted as shown in Fig. 3b. Due to symmetry in Fig. 3a, it is relatively easier to minimize the friction losses when the heavy masses are lifted vertically along the passage.

Fig. 3 also shows the carbon brushes which contact the vertical conductors spreading from the bottom to the top of the passage. Between brushes and terminals of the rotor conductors there are converter circuits described in a later paragraph. Such brush structure can also be applied to the configuration in which full magnetic stator structure or non-interleaved stator structure is used as mentioned in [7].

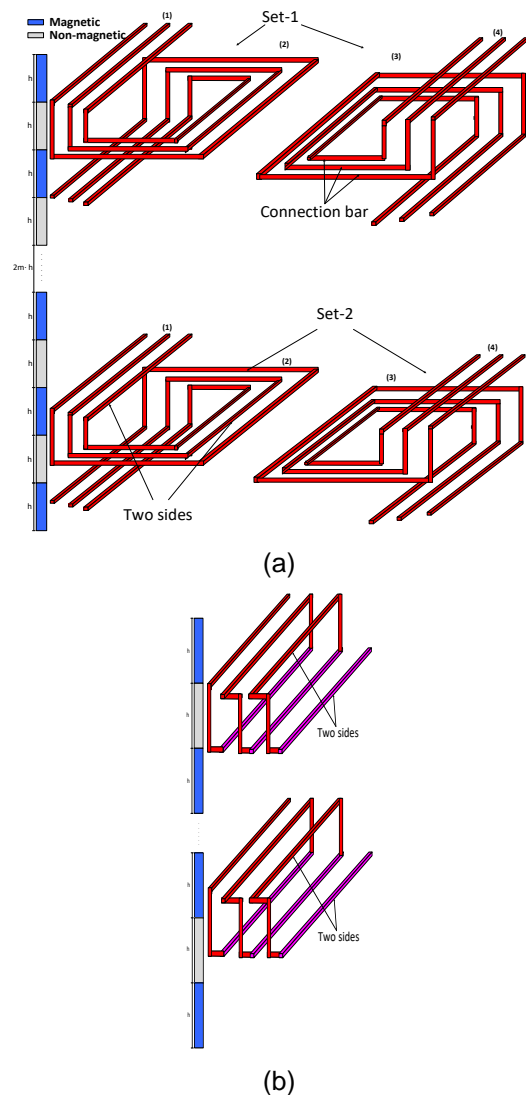


Fig. 2. (a) First way to wind the winding; (b) Second way to wind the winding

Fig. 4 shows vertical cut cross section of a rotor structure with combined sets where each stator layer, either magnetic or non-magnetic one, accommodates two rows of the rotor conductors. Rows CRA1 and CRA3 are wound in the way as shown in Fig. 2b to form two sides of one coil with multiple turns. CRA2 and CRA4 are also wound in the way as shown in Fig.

2b to form two sides of another coil with multiple turns. Each of the coils is supplied with AC current to ensure the electromagnetic force always uplifting. CRA1-CRA3 is grouped into set 1; CRA2-CRA4 is grouped into set 2. There could be three rows or even more rows of the rotor conductors under one stator layer. By doing so, the rotor vertical span is shortened and it becomes more compact. Furthermore, by doing so, multiple rotors can be accommodated.

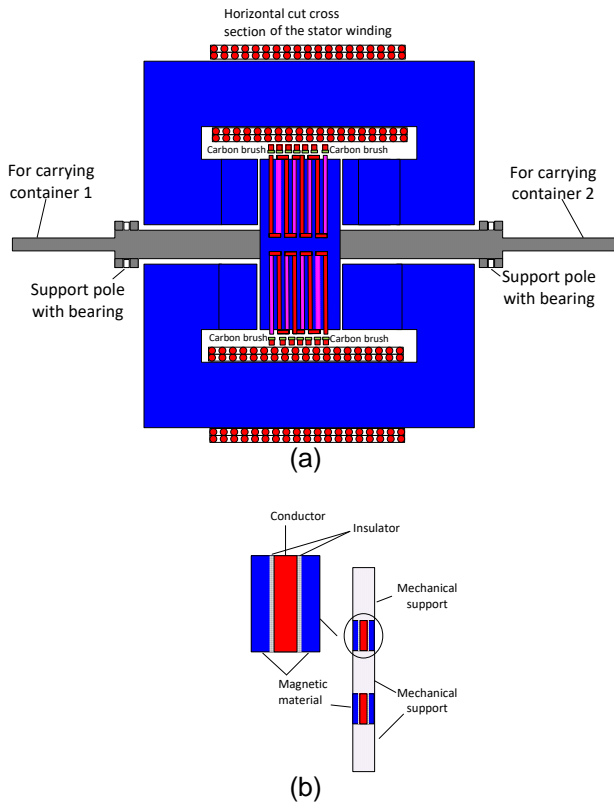


Fig. 3. (a) Horizontal cross section of the AC-DC induction machine; (b) Magnified basic rotor forming unit

The driving currents for the rotor conductors in Fig. 4 are shown in Fig. 5a and 5b. The currents in CRA1-CRA3 and CRA2-CRA4 conduct alternately to produce constant uplifting force. There are short-time over-laps of currents in two coils during transition as seen in Fig. 5a. The electromagnetic force produced by the currents in Fig. 5b is greater than that in Fig. 5a. Nevertheless the cross sectional areas of each rotor conductors for conducting the currents in Fig. 5b need be increased accordingly, and at each transition, the non-zero current of the corresponding coil needs to become doubled. Correspondingly rotor conductors need be designed to conduct not only its rated current but also a narrow pulse currents with amplitude as high as two times its rated current. As the pulse does not last long, this will not lead to too much increment of the rotor conductors' cross sectional area. Exact rotor conductor area increase can be determined by dynamic thermal modelling to ensure its one period of movement without incurring its temperature rise above limit, which is mainly determined by the insulators used in the system. As some insulators can bear temperature as high as 150 degree Celsius, slight

increase in cross sectional area may be sufficient. If one takes this approach, then more uplifting electromagnetic force is produced to lift heavier mass without incurring much change to the size of rotor conductors but at the sacrifice of system efficiency as higher operating temperature leads to higher copper losses.

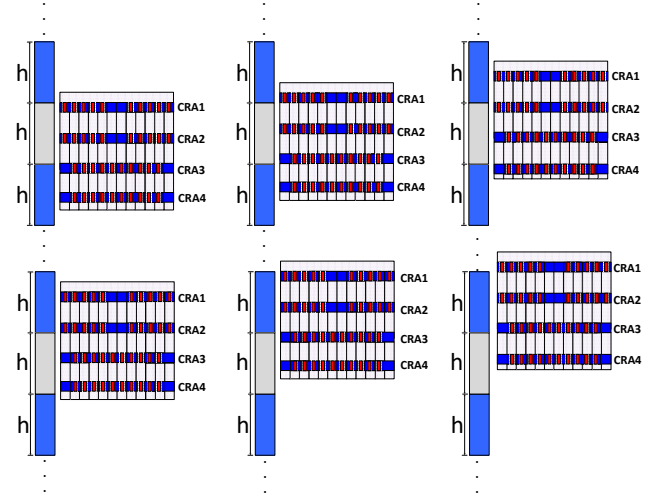


Fig. 4. Vertical cut cross section of rotor structure with combined sets where each layer accommodate two rows of rotor conductors

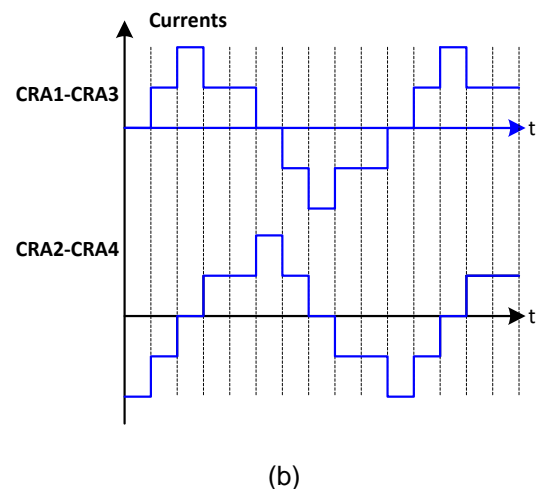
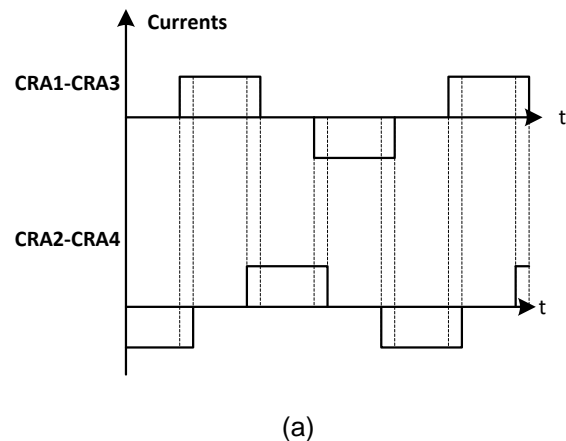


Fig. 5. Waveforms of currents flowing through rotor conductors with two rows of rotor conductors at each layer

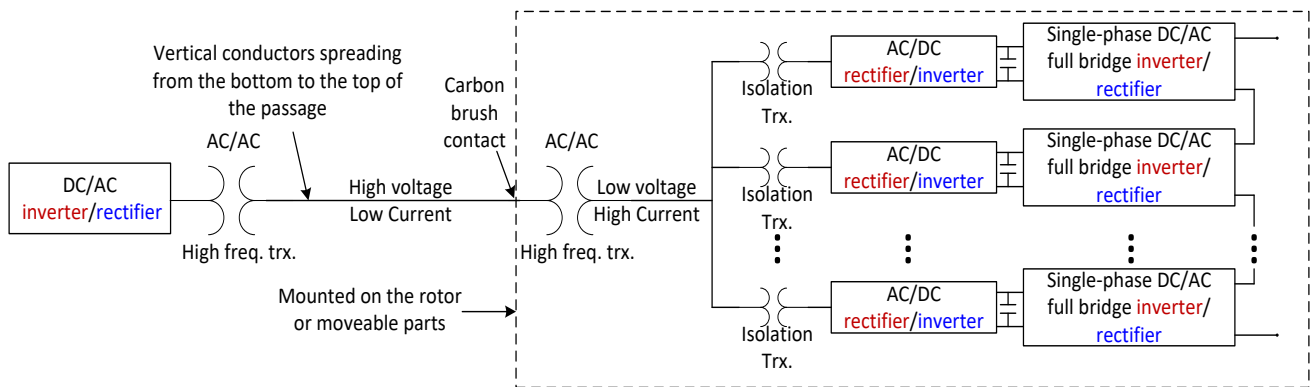


Fig. 6. Control circuit to generate drive/re-generation currents

To facilitate current change between $+I_{rated}$ or $-I_{rated}$ and 0 in Fig. 5a, and also sudden increment or decrement of currents between one time and two times of the rated currents in Fig. 5b, it is necessary to drive the rotor conductors with a periodic pulse voltage with high amplitude and very short rise/fall time, which could be achieved by connecting in series the outputs of multiple single-phase voltage-source full-bridge inverters as shown in Fig. 6. After producing the pulse voltage for facilitating the current change, the same circuit in Fig. 6 with much less stages is used to produce rated or nearly rated driving current and other stages are bypassed and produce zero voltage outputs. By doing so, the current waveforms in Fig. 5a and 5b can be obtained. For a practical application, one may divide the total rotor conductors into more groups with conductors in each group being connected in series. By doing so, the inductance of each group is reduced and the required pulse voltage for changing current magnitudes and/or directions is reduced as well. Nevertheless such approach will incur more currents flowing through the conductors spreading from the bottom to the top of the passage.

Special attention needs be paid when the transition happens. This is because the top and bottom side of one coil may experience opposite force simultaneously right before or after the transition.

Such effect compromises the effective lifting force. One solution is to stop the current flowing before sides of coil move close to the boundary and delay supplying current after the coils move away from the boundary. A de-rating factor needs be applied in the design to address this effect.

Fig. 7a shows stainless steel support for one row of the rotor conductors for the symmetrical structure as shown in Fig. 3a; Fig. 7b shows side view of the case for holding the rotor conductors sandwiched in magnetic materials through insulators; while Fig. 7c shows rotor conductors sandwiched in magnetic materials and separated by insulators, partly inserted in the casing in Fig. 7b. Fig. 7c also contains long bolt-nut made of stainless steel between side A1 and side B1. There are view separation curves in Fig. 7a, which correspond to the curves in Fig. 7b. This is for

simplifying the 3-D drawing in Fig. 7a. Many parallel flat rotor conductors protrude at both terminals, from which multiple rows of the rotor conductors are connected in either of the two ways as shown in Fig. 2.

To increase mechanic strength, another casing structure, slightly different from that in Fig. 7a and Fig. 7b by having central protrusions is shown in Fig. 7d and Fig. 7e, which are bottom and top of the casing respectively. These two parts are joined by bolt-nut or other joining mechanism through seven protruding parts in Fig. 7d. An illustrative part of the rotor conductors sandwiched in magnetic materials through insulators is shown in Fig. 7f, where central curving for the conductors is adopted to save space for central stainless steel protrusion as shown in Fig. 7d. In the curving part, rotor conductors are only separated by insulators and with no magnetic materials. Fig. 7g shows partly assembled rotor conductors and casing bottom. To save cost on the stator magnetic material, a corresponding stator is shown in Fig. 7h, where non-magnetic strip is adopted in the stator magnetic layer.

The casing structure given in Fig. 7d to Fig. 7g is also applicable to the distributed rotor case.

Fig. 8 shows stainless steel links and supports for joining two neighbouring units of the rotor structure as shown in Fig. 7. These links and supports are installed on the structure as shown in Fig. 7a.

Fig. 9 illustrates one example design of rotor structure with container carrier and mechanic hangers for hanging the containers. Two identical containers are lifted each time. There are two poles spreading from the bottom to the top of the passage, along which the rotors move. In practice, four such poles could be used for better stability. Bearings are installed to ensure smooth movement of the rotors along the support poles.

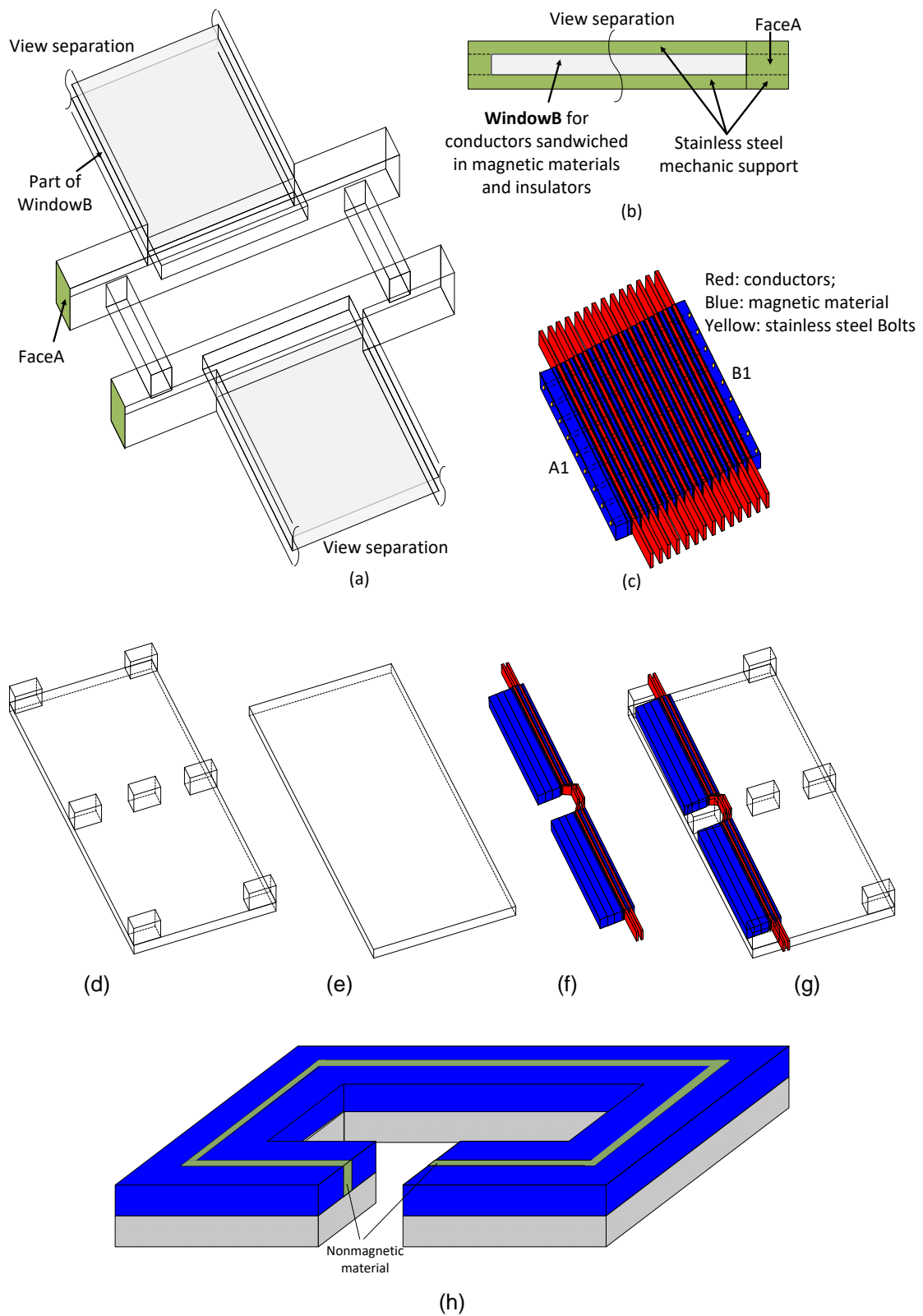


Fig. 7. Basic forming units of the row structure (a) stainless steel support for one row of the rotor conductors; (b) side view of the case for holding the rotor conductors sandwiched in magnetic materials; (c) rotor conductors sandwiched in magnetic materials and separated by insulators; (d)-(g) disassembled stainless steel casing for accommodating rotor conductors sandwiched in the magnetic material through insulators with central stainless steel reinforcement; (h) interleaved stator structure with non-magnetic strip to suit the rotor arrangement in (d)-(g)

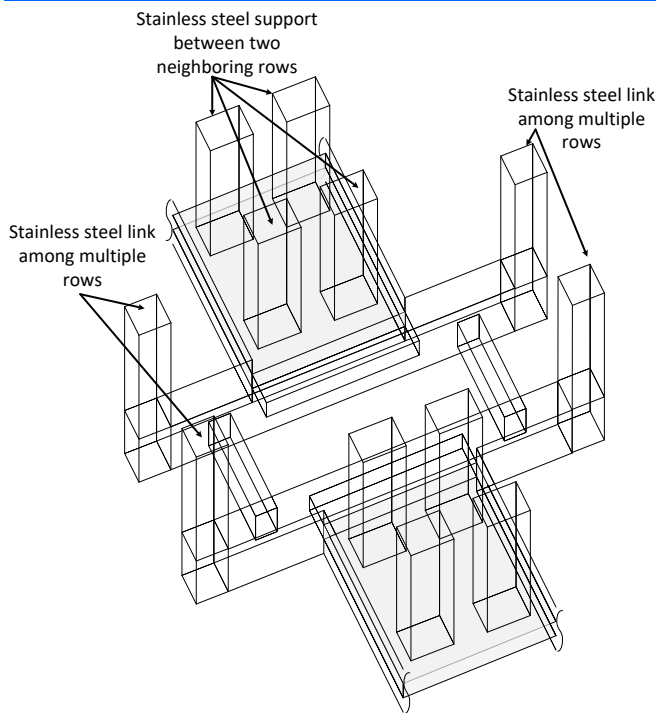


Fig. 8. Stainless steel support for one row of the rotor conductors in Fig. 7a with stainless steel link for neighbouring rows of the rotor conductors

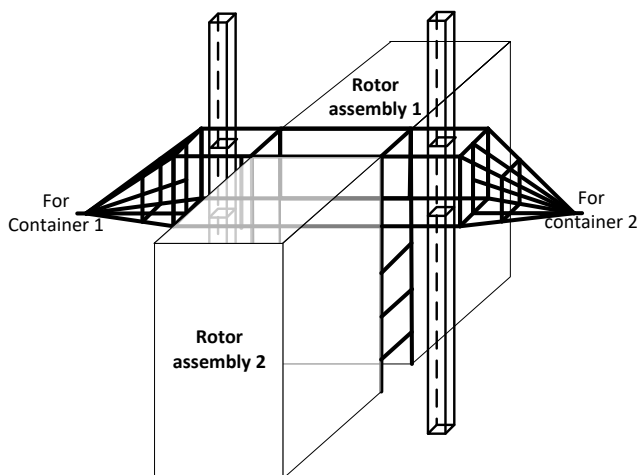


Fig. 9. One example of overall lumped rotor structure with mechanic hangers for hanging the containers

III. RE-CONFIGURABLE ROTOR STRUCTURE

In the AC-DC linear machine described above, the total force acting on the rotor can be expressed as

$$F_{tot} = F_s + F_{rs} + F_r \quad (1)$$

where F_s is reluctance force produced by the stator, F_{rs} is the electromagnetic force due to the interaction between rotor current and magnetic flux produced by the stator current, and F_r is reluctance force produced by the rotor.

As described in [7], in order to make reluctance force F_r always upward pointing, a new re-configurable rotor structure can be arranged and

shown in Fig. 10. Its working mechanism is summarized below [7].

For the upward movement at position (a) in Fig. 10, S11-S12 form one coil with current flowing through it to produce uplifting force while S13 serves as one separate side which also has current flowing through it to produce uplifting force. S22-S23 form another coil with current flowing through them to produce uplifting force while there is no current flowing through S21 which is separated from S22 and S23. By doing so, the reluctance forces by both S11-S12 and S22-S23 point upward. They will enhance the electromagnetic force F_{rs} . This can maximize the total uplifting forces. In position (b) in Fig. 10, coils are re-configured. S12-S13 form one coil with current flowing through them to produce uplifting force while there is no current flowing through S11 which is separated from S12 and S13. Now S21-S22 form one coil with current flowing through it to produce upward pointing force. S23 serves as one separate side with current flowing through it to produce uplifting force. By doing so, the reluctance forces by both S12-S13 and S21-S22 point upward and enhance the electromagnetic force F_{rs} . Coming to position (c), it repeats that in position (a). That is to say, S11-S12 form one coil, S22-S23 form another coil, S13 with current flowing through it to produce uplifting force, no currents flowing through the separate side S21. Fig. 10d shows the magnified re-configurable rotor structure.

Fig. 11 shows the 3-D arrangement of the three-sided rotor conductors. It is only for coils S11-S12-S13 and S31-S32-S33 in Fig. 10. Fig. 11b illustrates the conducting currents and switches' connections for the movement from position in Fig. 10a to position in Fig. 10b. Fig. 11c shows the conducting currents and switches' connections for the movement from position in Fig. 10b to position in Fig. 10c. Configuration in Fig. 11d repeats that in Fig. 11b.

Switches in Fig. 11 can be power switches such as IGBT, MOSFET, thyristors or others. Such switching could also be achieved by using carbon brush based commutation as shown in Fig. 12a, where multiple brushes are mounted on a belt, pulled by the rotating wheels which are driven by motors. Three terminal connections such as SW2, or SW51 or SW52 in Fig. 11a are illustrated. In one duration, T1 and T2 are connected just like that in Fig. 11b while in next following duration, T2 and T3 are connected, just like that in Fig. 11c. In Fig. 11, there are only two turns illustrated. Correspondingly there are two sets of T1-T2-T3. For a practical application, many more turns are used and correspondingly there is the same number of sets of T1-T2-T3. One may modify that in Fig. 12a to suit two-terminal switches such as SW31 and SW32. In such kind of brush commutation, instead of moving conductors as in conventional DC machine, the conductors stand still relative to the rotor structure while brushes are driven by the rotating wheels and move along with the belt.

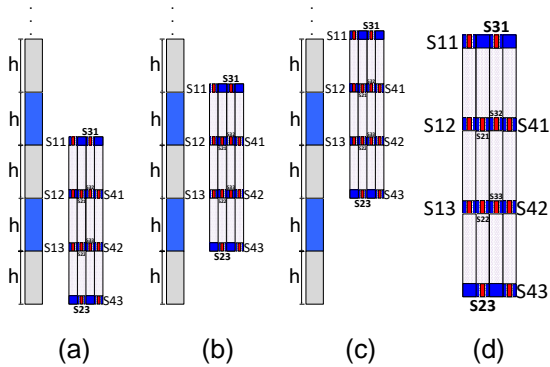


Fig. 10. An arrangement of rotor conductors to use EM and reluctance forces simultaneously

Fig. 12b shows the drive circuit for providing DC currents into S13 and S33 from position in Fig. 10a to that in Fig. 10b or into S23 and S43 from position in Fig. 10b to that in Fig. 10c. As there are conductors from multiple rows to form multiple parallel circuits, correspondingly there are multiple outputs in the circuit as shown in Fig. 12b.

Although re-configurable structure makes movement smoother and comes with more lifting force, its implementation is much more complicated.

It is still possible to use multiple groups of parallel conductors to form complete rotor structure. All those rows of rotor conductors under the stator magnetic layer are fed with currents to produce uplifting forces

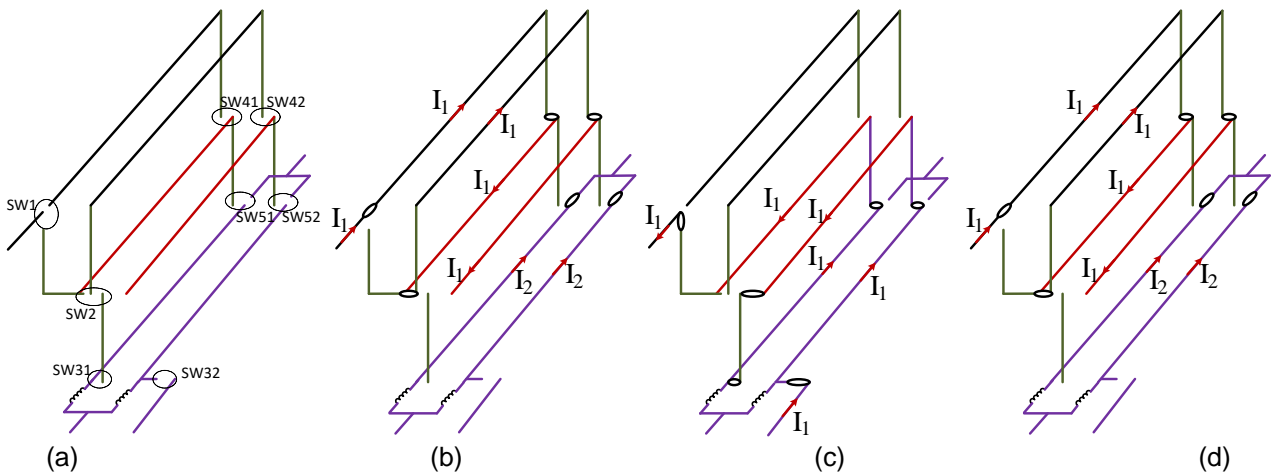


Fig. 11. Configuration of three-sided rotor conductors

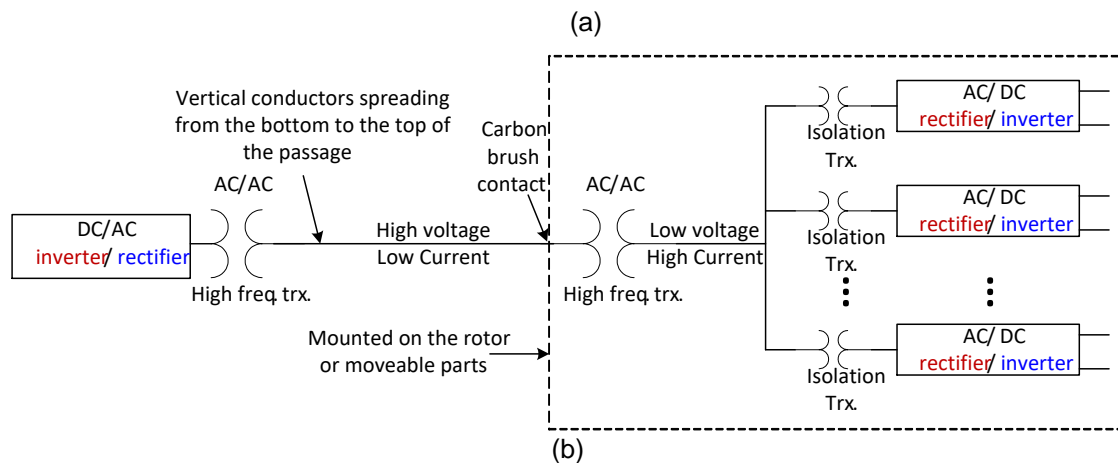
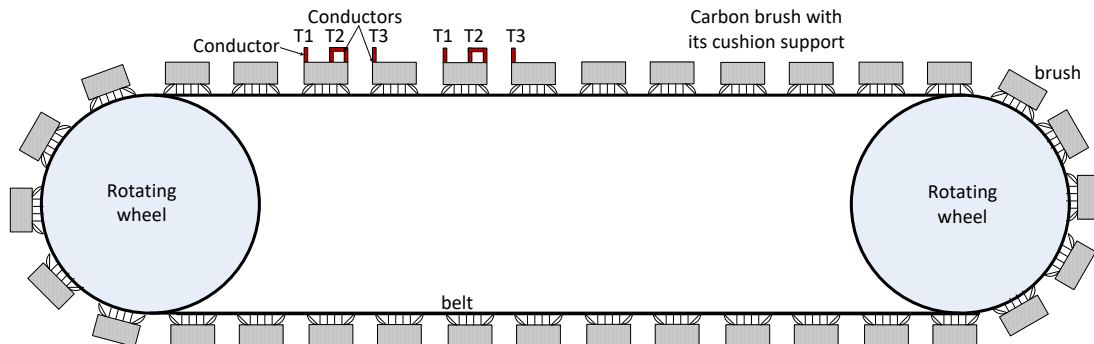


Fig. 12. (a) Rotating mechanism to achieve switching function; (b) Drive circuits for the parallel conductors

while other groups of rotor conductors under the stator non-magnetic layer have no current flowing through it. Then multiple drive circuits as in Fig. 12b need be used. Nevertheless such structure may suffer circulating currents issue in the rotor conductors as it is hard to keep the magnetic field in the air gap under the magnetic layer uniform experienced by the rotor conductors. This issue will be further addressed in a later paragraph.

One may use the basic configuration as shown in Fig. 4 to achieve the lifting of heavy masses. By using pulse current waveform as shown in Fig. 5b, the effective lifting force is enhanced. In the following design with multiple rotors, such structure is used.

IV. EXAMPLE DESIGN WITH MULTIPLE ROTORS

As wind is intermittent, it is necessary to have multiple rotors to lift more heavy masses at one time within a short duration.

The example design with two rotors is shown below.

Table 1 through Table 7 shows the information of the design. In this design two rows of rotor conductors under one stator layer for each of two rotors are adopted, the same as that in Fig. 4. The current conducting technique shown in Fig. 5b is taken.

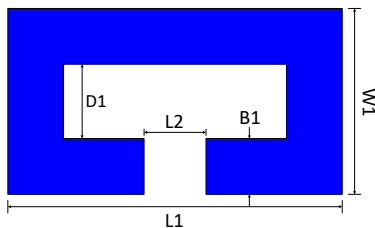


Fig. 13. Dimensions of the magnetic structure for the stator (cross sectional view)

The following is the temperature-current equation for the conductor,

$$\left(\frac{I_2}{I_1}\right)^2 = \frac{T_2 - T_a}{T_1 - T_a} \quad (2)$$

where I indicates current, T temperature, and a ambient.

According to the above equation, there could be quite high temperature rise if the current becomes higher than rated one.

The rated current for the rotor conductors is 500A in this design. Assume that the current flowing through each one is equal to 80% of the rated current or 400A when both rows of the rotor conductors produce uplifting force. When one row of the rotor conductor is under transition at the boundary between magnetic and non-magnetic layers, the other needs to conduct 800A current to produce the same lifting force, which is 1.6 times its rated current. By doing so, the rotor temperature rise during transition is made acceptable. For such a design the height of the rotor is around 25m.

To make the system more compact, one may use three or more rows of rotor conductors under one layer. For example, assume that three rows are taken. Under normal operation, each one takes 80% of its rated current. When one experiences transition, the other two take 120% of the rated currents to produce the same lifting force. By doing so, the temperature rises can be mitigated. For such a design, the height of each rotor can be shortened to be around 17m. When one layer accommodates more rows of the rotor conductors, the connection of the terminals of the rotor conductors becomes more complicated.

To examine how the fringing effect is in both lumped rotor structure and distributed rotor structure [7], a simplified structure is taken and shown in Fig. 14.

Fig. 14 shows the two mimicking configuration of the rotor structure, one being distributed rotor in Fig. 14a while the other being lumped rotor in Fig. 14b. Figure 14c shows the distributed rotor structure with five lines defined for observing the magnetic fields.

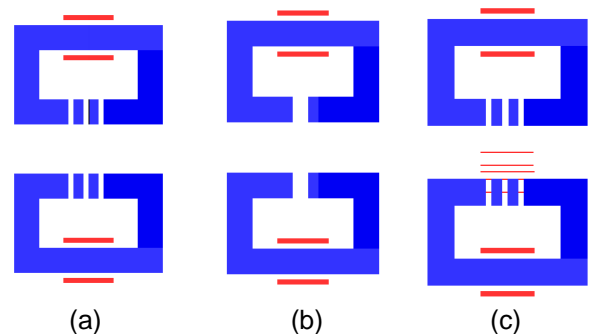


Fig. 14. (a) Distributed rotor; (b) lumped rotor; (c) Distributed rotor with five lines defined for observing magnetic fields (From top to bottom: Line 1, Line 2, Line 5, Line 3 and Line 4)

Fig.15 and Figure 16 are the magnetic field distributions along the five lines defined in Fig. 14c. From these two figures, one can see that the magnetic field distributions along lines 1, 2 and 5 for the distributed rotor structure are pronouncedly lower than those for the lumped rotor structure. Hence the distributed rotor structure is a better choice for reducing EM force de-rating effect and having more stable movement of the rotor system.

Another effective way to mitigate such effect is to increase the width of the core B1 in Fig. 13 thereby increasing length of the rotor conductors which experience electromagnetic forces. By doing so, less number of flat rotor conductors is required and correspondingly the air gap is reduced. Nevertheless such approach incurs more use of stator magnetic materials.

From Table 4, one can see that the air gap of the rotor is 0.32m and the total width of the rotor L2 in Fig. 13 is around 0.64+0.006=0.646m, where 6mm is left for the two gaps between rotor and stator. To reduce fringing effect, one can increase the core width B1 thereby reducing the rotor air gap. By doing so, the

electromagnetic force de-rating effect during transition at boundaries between magnetic and non-magnetic materials can be mitigated. Alternatively, distributed rotor structure sandwiched in mechanic support reinforced interleaved stator magnetic plates as shown in Fig. 17a can be taken. Then one can divide the total 64cm of rotor span into eight parts, each being 8cm, which is installed in the similar casing as in Fig. 7a with the central protrusion as in Fig. 7d and is still mechanically strong enough to counterbalance the electromagnetic force acting on the rotor conductors. At both terminals, all the eight parts are joined mechanically by stainless steel or other mechanically strong materials. To have better mitigation of the fringing effect, wider interleaved stator plates are used. Fig. 17b and Fig. 17c show an example with four distributed rotors. In between them, there are interleaved stator plates.

The distributed rotor structure as shown in Fig. 17 can be adopted for re-configurable rotor structure as well.

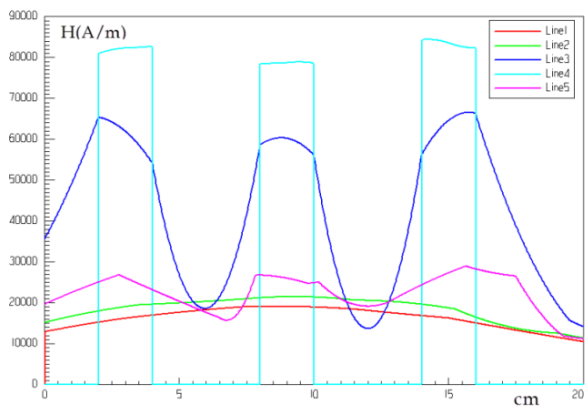


Fig. 15. Magnetic field distribution along five lines in the distributed rotor

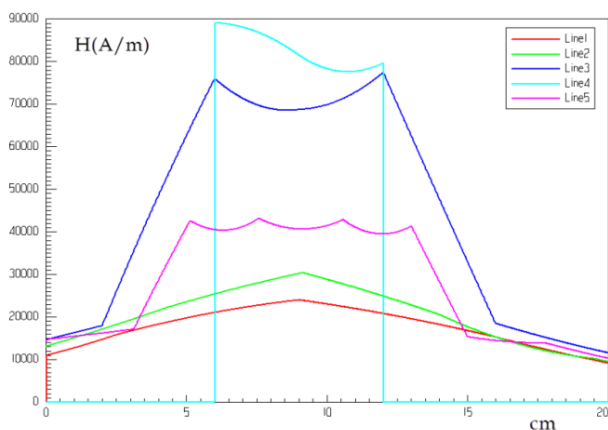


Fig. 16. Magnetic field distribution along five lines in the lumped rotor

Since the stator magnetic cores work in a minor loop of magnetization, demagnetization is needed for an efficient operation. Furthermore the minor problem of armature reaction due to the currents in the rotor conductors needs to be considered for a detailed design.

Table 1. Dimensions

Dimensions	m
Core width B1	0.8m
Core length L1	2.95m
Core inner space distance D1	3.89m
Height of the passage	200m
Alternate layers	200

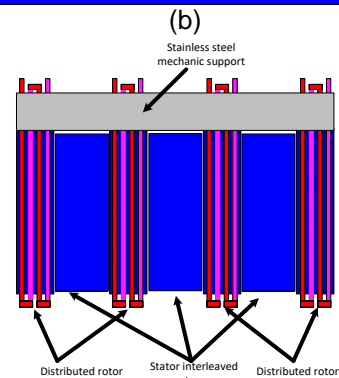
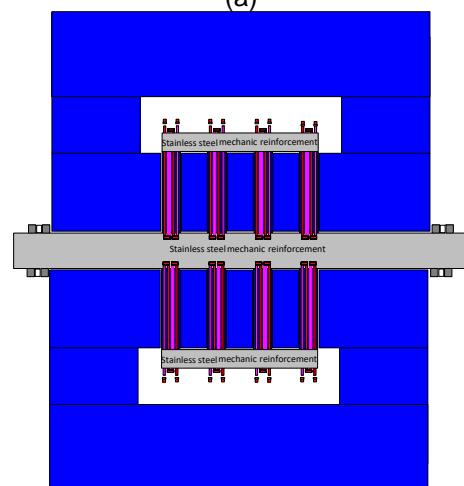
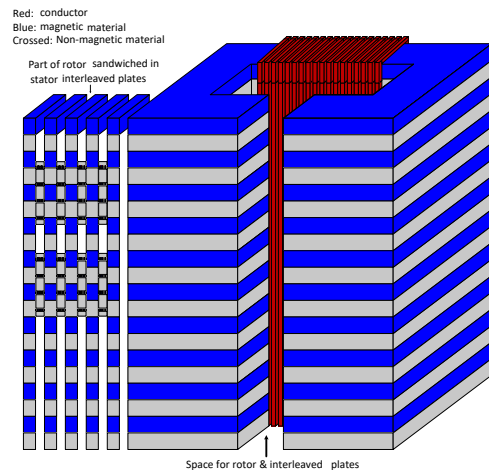


Fig. 17. A system with interleaved plates for reducing fringing effect in which distributed rotor structures are sandwiched (a) 3-D view; (b) top-view without showing stator conductors; (c) part of the structure in (b)

Table 2. Parameters

Air permeability	$4\pi \times 10^{-7}$ H/m
Saturation flux density	1.25 T
Steel density	8×10^3 kg/m ³
Copper mass density	8.96×10^3 kg/m ³
Copper conductivity	5.96×10^7 S/m
Aluminum conductivity	3.5×10^7 S/m
Stator current	500A
Rotor current	500A
Cross sectional area of individual stator conductor	3.5×10^{-4} m ²
Stator conductor increment factor	16
Total each stator conductor's area	$16 \times 3.5 \times 10^{-4}$ m ²
Cross sectional area of individual rotor conductor	3.5×10^{-4} m ²

Table 3. Material cost

Dimensions	m
Copper	0.65US\$/kg
Aluminium	2000US\$/m ³
Steel	600×8 US\$/m ³
Concrete or cement	30US\$/ton
Electricity tariff per kWh	0.20US\$;

Table 4. Rotor information

Rotor conductor pair per layer	4
Rotor conductor number per section	20
Total number of conductors per layer	$4 \times 2 \times 20 = 160$
Number of rows of rotor conductors per stator alternate layer	2
Rotor conductor coil number (formed by two rows of the conductors)	10
Conductor	Copper
Thickness of rotor conductor	2mm
Air gap in rotor	0.32m $= 2\text{mm} \times 160$
Width of the rotor (L2 in Fig. 13)	0.64m
Travel speed of the rotor	6.0m/s
Number of rotors	2
Height of each rotor set	$2 \times 10 = 20\text{m}$

Table 5. More information

Number of containers	2000
Loss factor	2.0
Cost factor	2.0
Mass per container	$114.10/2 = 57.5\text{ton}$

Yearly usage rate	80%
Total energy stored	175.33MWh

Table 6. Breakdown construction cost

Parts	Million dollars
Steel	5.4044
Heavy mass	5.448
Copper for the rotor	0.1044
Aluminum for the stator	1.5680
Total Cost	$2 \times 25.05 = 50.10$

Table 7. Losses and efficiency

	kW
Power losses in the rotor	86.29
Power losses in the stator	714.29
Power at 6m/s	13440
One-way efficiency	93.40%
Round-way efficiency	87.24%

In the structure where the rotor is formed by multiple circuits each of which is formed by a number of parallel conductors, fringing effect must be addressed as well to avoid severe circulating currents. In such a structure, it is also good to use distributed rotor with interleaved stator plates. Figure 18 shows such an arrangement, where conductors 1a, 1d, 2a, 2d, 3a, 3d, 4a and 4d are connected in parallel while the conductors 1b, 1c, 2b, 2c, 3b, 3c, 4b and 4c are connected in parallel. Such arrangement is necessary since induced voltages in conductors 1a, 1d, 2a, 2d, 3a, 3d, 4a and 4d are nearly the same due to the field distribution pattern. Similarly induced voltages in the conductors 1b, 1c, 2b, 2c, 3b, 3c, 4b and 4c are also nearly the same. By doing so, circulating currents could be well contained. For the case where there are more conductors in one distributed rotor, symmetry rule as adopted for the four conductors in one distributed rotor in Fig. 18 is still applicable and even number of the rotor conductors in one distributed rotor is taken. Such symmetry arrangement is also applicable to the re-configurable rotor structure as shown in Fig. 10, where S11-S12-S13 and S31-32-33 can be arranged at two sides while S21-S22-S23 and S41-S42-S43 are arranged at the center, sided by S11-S12-S13 and S31-32-33.

Such rotors with multiple paralleled rotor conductors are comparable to the structure as given in Fig. 4. The structure in Fig. 18 can contain multiple rows of the rotor conductors as in Fig. 4. The number of rows of the rotor conductors under one magnetic layer of stator is the same as that of the rows of the rotor conductors under one non-magnetic layer of stator. Each time, when one row of the rotor conductors enters the magnetic layer, the current is fed through it by the circuit in Fig. 12b. When the row of the rotor conductors leaves the magnetic layer and enters the non-magnetic layer, the current flowing through it is forced to be zero to avoid the counteracting EM force.

As field at Line 3 and Line 4 as shown in Fig. 14c are different, it is preferable to have only conductors in parallel from the same row.

Nevertheless rotor structure with multiple parallel conductors needs to draw very high current. For the design shown in [7], one row contains 160 rotor conductors. Each one carries 500A. If one uses the parallel-rotor-conductor approach, the total currents drawn by one row of rotor conductors are $500A \times 160 = 80,000A$. Furthermore, there are multiple rows of rotor conductors to lift the heavy mass. To suit such high current application, there should be multiple circuits as that in Fig. 12b. Theoretically rotor structure with multiple circuits each of which is formed by paralleled conductors is possible but practically there are several technical obstacles to overcome, including 1) The AC/AC transformer in Fig. 12b in each circuit after the carbon brush needs to work at very high frequency. Otherwise, total weight of multiple such transformers will ruin the design as they may make the rotor system too heavy; 2) when the high voltage and low current conductors spreading from the bottom to the top of the platforms carry very high-frequency current, requirement on brush contacts is very high. Currently there may be no such technology; 3) multiple isolation transformers in each circuit take quite much weight as well. This further reduces the ratio of heavy mass weight lifted by the linear machine to the rotor mass weight; 4) there are quite many converter circuits and switches which reduce system reliability.

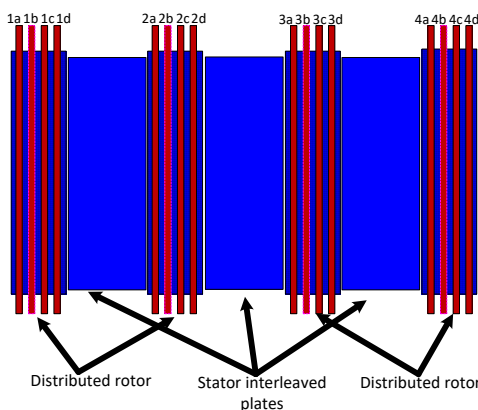


Fig. 18. Distributed rotor structure with multiple paralleled rotor conductors and interleaved stator plates

The container could be stainless steel framed and plastic windowed configuration. The heavy mass could be conventional concretes, bricks etc to save cost.

In practice, the most suitable design is the distributed rotor structure with interleaved stator plates, in which the rotor conductors are divided into several groups, within each of which all the conductors are connected in series as shown in Fig. 2a or Fig. 2b. With such a design, the profit return years could be less than nine years. Projected life

span for the main components could be as long as 50 years.

By using more rotors, moving efficacy can be enhanced. That is to say, within the same duration, more containers can be moved and more energy stored.

V. CONCLUSION

This paper presented a heavy mass energy storage system using an AC-DC linear machine, which lifts heavy masses vertically. By using multiple parallel stator conductors wound on the interleaved stator structure, ohmic losses in them are effectively reduced. Moreover by having symmetrical structure and vertical movement, the friction due to rotor movement is minimized. Furthermore two rotors are adopted to increase lift efficacy and shorten lifting time, thereby making it more suitable for intermittent and short-lasting wind energy storage. From calculation, it is predicted that the profit-return year could be less than nine years and round-way efficiency is above 85%.

To positively use reluctance force, this paper proposed to use three-sided or reconfigurable rotor topology. By doing so, the movement of the rotor is made smoother. Nevertheless such system is more complicated to implement and control.

To reduce the fringing effect during the transition of the rotor between interleaved layers of the stator structure, interleaved stator plates are used to sandwich the distributed rotors. By doing so, fringing effect induced de-rating on the electromagnetic force could be mitigated.

REFERENCES

- [1] Daniel E. Olivares, and Nikos D. Hatziargyriou, "Trends in Microgrid Control", IEEE TRANSACTIONS ON SMART GRID, VOL. 5, NO. 4, JULY 2014, pp.1905-1919.
- [2] N.W.A. Lidula, A.D. Rajapakse, "Microgrids research: A review of experimental microgrids and test systems", Renewable and Sustainable Energy Reviews, vol.15, JAN 2011, p.188.
- [3] Alan J. SANGSTER, "Massive energy storage systems enable secure electricity supply from renewables", J. Mod. Power Syst. Clean Energy (2016) 4(4), pp.659-667.
- [4] UWilliam R. Peitzke, TMatthew B. Brown, William L. Erdman, Robert T. Scott, William H. Moorhead, Douglas C. Blodgett, David I. Scott, Utility Scale Electric Energy Storage System, USA patent, No.: US 8,593,012 B2.
- [5] Daniel N. Boone, ENERGY WEIGHT STORAGE, USA patent, No.: US 2016/0138572 A1.
- [6] Tom Scott, ViewTekz LLC., "ENERGY STORAGE", USA patent, US 7,973,420 B2.
- [7] Daming Zhang, "Review on Heavy Mass Energy Storage and a New Such a System Using Interleaved Magnetic Structure", AUPEC 2018, Auckland, New Zealand, pp. 1-8.